JOURNAL OF CATALYSIS 117, 246–257 (1989)

Reduced Molybdenum Formal Oxidation States in Hydrodesulfurization Catalysis by Chevrel Phases

M. E. EKMAN, J. W. ANDEREGG, AND G. L. SCHRADER[1]

Department of Chemical Engineering and Ames Laboratory, U.S. Department of Energy, Iowa State University, Ames, Iowa 50011

Received June 3, 1988; revised December 22, 1988

The effect of the oxidation state of molybdenum on the catalytic hydrodesulfurization (HDS) of thiophene was investigated using a series of lead–lutetium Chevrel phases. Polycrystalline catalysts were prepared with compositions of $PbMo_{6.2}S_8$, $Lu_{1.2x}PbMo_6S_8$ for $0 < x \leq 0.2$, and $Lu_{1.2x}Pb_{1-x}Mo_6S_8$ for $0.2 < x \leq 1$. Fresh and used (10-h thiophene reaction) catalysts were characterized by X-ray powder diffraction, laser Raman spectroscopy, and X-ray photoelectron spectroscopy. Bulk structures and molybdenum oxidation states were found to be stable. HDS activity could be related to the molybdenum formal oxidation state: the maximum rate of thiophene HDS was observed for catalysts having "reduced" oxidation states (compared to MoS_2). All Chevrel phase catalysts demonstrated low activity for 1-butene hydrogenation.

INTRODUCTION

Typical industrial catalysts used in hydrodesulfurization (HDS) processes are prepared from alumina-supported molybdenum (Mo^{6+}) oxides which are promoted with cobalt or nickel to improve catalytic activity (*1–3*). The oxides become sulfided and reduced under catalytic reaction conditions. The presence of a MoS_2 (Mo^{4+}) phase has been demonstrated by various researchers using techniques such as X-ray photoelectron spectroscopy (*4–6*), EXAFS (*7*), X-ray diffraction (*8*), and laser Raman spectroscopy (*9*). Numerous studies of unsupported HDS catalysts have also been performed in an attempt to model supported materials. Using X-ray photoelectron spectroscopy (XPS), it has been shown that MoS_2 is formed from cobalt–molybdenum–oxygen catalysts after treatment at 400°C with H_2/thiophene or H_2/H_2S (*10*). MoS_2 is an active HDS catalyst with properties similar to those of supported catalysts (*11*). Topsøe *et al.* (*12*) have reported the existence of a cobalt–molybdenum–sulfide (Co–Mo–S) phase in both supported and unsupported molybdenum HDS catalysts as determined from Mössbauer emission spectroscopy. This phase is proposed to be the active material involved in industrial HDS catalysts, based on the existence of a linear relationship between the amount of cobalt in the Co–Mo–S phase and catalytic activity (*2*). The phase is considered to be a MoS_2-like material in which promoter atoms occupy crystallite edge positions (*13*).

The role of "reduced" molybdenum oxidation states (lower than the +4 state of MoS_2) in HDS has not been clearly established. Several techniques have been used to investigate the nature of the active molybdenum species. For example, XPS measurements for unsupported, sulfided cobalt–molybdenum catalysts have demonstrated a decrease in the molybdenum 3*d* binding energies for cobalt concentrations corresponding to the maximal promotional effect for thiophene HDS (*14*). From this information, it was postulated that reduced molybdenum species with a charge between +3 and +4 are associated with the active sites. Alstrup *et al.* (*15*) have also used XPS to study supported and unsupported Co–Mo catalysts. They found a close similarity

[1] To whom correspondence should be addressed.

0021-9517/89 $3.00

between the Co 2*p* spectra of Co–Mo–S and $CoMo_2S_4$ and suggested that the electronic state of Co in Co–Mo–S was similar to that in $CoMo_2S_4$ (which has a formal molybdenum oxidation state of +3). The two phases are structurally different, however.

Other investigators have deduced the presence of Mo^{3+} and W^{3+} species on supported and unsupported Co–Mo, Ni–Mo, and Ni–W sulfide catalysts using electron paramagnetic resonance (EPR) techniques. Voorhoeve (*16*) utilized EPR in the investigation of the hydrogenation of benzene using WS_2 (MoS_2) catalysts and concluded that the active centers were W^{3+} (Mo^{3+}) ions. Konings *et al.* (*17*) have observed a correlation between the intensity of an EPR signal attributed to Mo^{3+} and the rate of thiophene HDS for supported cobalt-promoted molybdenum catalysts. Thakur and Delmon (*18*) investigated unsupported promoted molybdenum and tungsten catalysts and detected the presence of Mo^{3+} and W^{3+} species: catalysts having the highest EPR signal also had the greatest HDS activity.

Adsorption studies have also been performed to characterize reduced molybdenum oxidation states on HDS catalysts. Bachelier *et al.* (*19*) and others (for example (*20–22*)) have demonstrated a relationship between the chemisorption of O_2, CO, or NO and HDS activity. A study of the chemisorption of O_2 and NO on a reduced and sulfided supported molybdenum catalyst was interpreted in terms of chemisorption on Mo^{2+} centers (*23*). Site-selective adsorption of CO has been proposed to occur on highly reduced molybdenum sites for both $Mo/\gamma\text{–}Al_2O_3$ (*24*) and $Co\text{–}Mo/\gamma\text{–}Al_2O_3$ catalysts (*25*); these sites were associated with HDS activity. Peri (*26*) reported CO and NO adsorption studies for supported molybdenum catalysts and interpreted the results as indicating the presence of exposed Mo^{3+} or Mo^{2+} sites. Laine *et al.* (*27*) explained their observations for NO adsorption on supported molybdenum catalysts promoted with both cobalt and nickel in terms of a minor reduction of Mo below the +4 oxidation state.

The complexity of the typical industrial catalysts—and even the uncertainties associated with unsupported catalysts—has made identification of reduced molybdenum oxidation states difficult. Due to the presence of a large amount of MoS_2 (or other related phases with predominantly Mo^{4+} oxidation states) in these catalysts, the role of reduced molybdenum states may be difficult to study.

Theoretical investigations, however, have indicated that reduced molybdenum oxidation states are involved as the active sites in HDS. Duben (*28*) has provided support for the existence of an active Mo^{3+} species using simple Hückel theory. According to his calculations, this oxidation state would be the most effective for carbon–sulfur bond breaking and would allow for easy removal of the surface bound sulfur atom to regenerate the active site. Harris (*29–30*) and Harris and Chianelli (*31–32*) have discussed molecular-orbital calculations for the electronic structures of MS_6^{n-} clusters (first- and second-row transition metals (*M*)) and promoted molybdenum clusters, $MoMS_9^{n-}$. Calculated trends in electronic factors and bonding were related to dibenzothiophene HDS activity to establish an electronic explanation for catalytic activity. Promoters such as Co or Ni transfer electrons to molybdenum so that the molybdenum formal oxidation state is reduced (relative to MoS_2). For a cluster containing Cu (a metal which poisons the activity of MoS_2-based catalysts), molybdenum is oxidized relative to MoS_2.

In recent years we have reported the results of HDS studies with reduced molybdenum sulfides known as Chevrel phases (*33–38*). Chevrel *et al.* (*39*) reported the initial synthesis and characterization of these ternary molybdenum chalcogenides in 1971. Chevrel phases have a general formula $M_xMo_6Z_8$, with *Z* being sulfur, selenium, or tellurium and with *M* being a ternary metal component. The Chevrel phase

structure can be described as a stacking of Mo_6Z_8 building blocks or clusters which incorporate the ternary metal cations in channels or voids created by the chalcogen atom network. When M is a large cation, such as Pb or Sn, a second component such as a rare earth (RE) may be incorporated to produce a series of compounds with nominal formulas $RE_xM_{1-x}Mo_6S_8$. Extensive reviews concerning Chevrel phases have been provided (*40–43*). In our research, Chevrel phases have been shown to have high activity for thiophene HDS (*33–35, 38*). The solid state chemistry of Chevrel phases offers an opportunity to investigate the effect of the oxidation state of molybdenum on HDS activity. Direct preparation of catalysts with reduced molybdenum oxidation states (compared to MoS_2) is possible. The formal oxidation state of molybdenum can be varied by using Chevrel phases with different compositions and/or ternary elements. The results reported here deal with a series of lead–lutetium Chevrel phase catalysts.

EXPERIMENTAL METHODS

a. Catalyst Preparation

The Chevrel phases were prepared by solid state synthesis from mixtures of: 200 mesh powdered molybdenum metal reduced at 1000°C in hydrogen for 18 h; sulfides of lead and lutetium which were made by direct combination of the elements in evacuated, fused-silica tubes; and powdered sulfur. The mixtures were ground together thoroughly, pressed into 13-mm pellets, and sealed in evacuated fused-silica tubes back-filled with argon to 20-in. Hg vacuum pressure. The tubes were heated slowly in a muffle furnace from 450 to 750°C over a period of 48–72 h, transferred immediately to a high-temperature box furnace at 1225°C for 24 h, and quenched in air. The materials were reground in air, pressed into pellets, and reheated for 48 h at 1225°C. After the final heating, the tubes were opened in a nitrogen dry box where the pellets were lightly crushed. The 40–100 mesh portion was separated for use in the activity measurements, and a small amount was reserved for XPS analysis. All subsequent manipulations of the catalysts were performed in the dry box.

Some differences concerning the exact stoichiometries necessary to obtain pure single phases of these materials exist in the literature. The content of the ternary element M is reported to be variable (e.g., $M_{1.0}Mo_6S_8$ and $M_{1.2}Mo_6S_8$ for the rare earth materials); the ratio of molybdenum to chalcogenide can also deviate from the "ideal" value of 6/8. Chevrel phases prepared at a nominal composition $M_{1.2}Mo_6S_8$ apparently are multiphasic, having a predominance of MMo_6S_8 with very small amounts of MoS_2, Mo_2S_3, and M-sulfides which cannot be detected by X-ray diffraction (*44*).

In this work, homogeneous polycrystalline samples were obtained for compositions prepared at $Lu_{1.2x}PbMo_6S_8$ for $0 < x \leq 0.2$ and at $Lu_{1.2x}Pb_{1-x}Mo_6S_8$ for $0.2 < x \leq 1$. A loss of lead is observed when x is greater than 0.2, demonstrating that there is a limit of rare earth insertion (*45*). It is necessary to prepare the lead compound with a composition of $PbMo_{6.2}S_8$ in order to obtain the purest single-phase material (*46*) containing about 1 wt% MoO_2 and less than 1 wt% of other impurities (MoS_2, Mo_2S_3) (*47*).

b. Activity Measurements

Hydrodesulfurization activities were measured at atmospheric pressure using a microreactor system (*33–35*). Catalyst loadings were adjusted to achieve less than 3% conversion of thiophene after 20 min of continuous reaction (ranging from 0.0795 g for $PbMo_{6.2}S_8$ to 0.4906 g for $Lu_{1.2}Mo_6S_8$). The reactor was heated from room temperature to 400°C in a flow of helium at 19 ml/min (STP). After 1 h at 400°C with flowing helium, ten 0.25-ml pulses of 2 mol% thiophene in hydrogen were injected into the reactor at 30-min intervals. A continuous flow of 2 mol% thiophene in hydrogen at 22

ml/min (STP) was used to determine steady-state activity. After 10 h of continuous reaction, the reactor was purged and cooled in a stream of helium.

Activity measurements for the hydrogenation (HYD) of 1-butene to *n*-butane were performed as described previously (*33–35*). The reactor was filled with the same amount of fresh catalyst as in the HDS activity measurements and was heated from room temperature to 400°C in a flow of helium at 19 ml/min (STP). After it was held at 400°C in the stream of helium for about 1 h ("fresh catalyst"), two 0.10-ml pulses of 2 mol% 1-butene in hydrogen were injected into the reactor at 15-min intervals. Twenty-five 0.10-ml pulses of 2 mol% thiophene in hydrogen were then injected into the reactor, and the 1-butene pulses were repeated. A continuous flow of thiophene in hydrogen for 2 h at 22 ml/min (STP) followed. The reactor was purged with helium, and the 1-butene pulses were repeated.

Product separation and analysis was performed using a 12-ft *n*-octane/Porasil C column and an Antek Model 310 gas chromatograph equipped with a flame ionization detector. Peak areas were measured by a Hewlett–Packard 3390A integrator. Since *trans*-2-butene and 1,3-butadiene have the same retention times, these materials were combined in the data analysis.

c. Catalyst Characterization

The catalysts were characterized before and after 10 h of continuous thiophene reaction.

The surface areas of the catalysts were determined by the BET method with krypton as the adsorbate at liquid nitrogen temperature using a Micromeritics 2100E Accusorb instrument.

X-ray powder diffraction patterns were acquired with a Siemans D500 diffractometer using Cu$K\alpha$ radiation. Samples were mounted on double-sided adhesive tape and scanned in the 2Θ range from 10 to 50 with a count of 1.0 s and step size of 0.04 2Θ.

Laser Raman spectra were recorded using a Spex 1403 monochromator and a Spectra Physics argon ion laser operating at 514.5 nm and 200 mW measured at the source. A Nicollet 1180E computer data acquisition system was used to accumulate 50 scans at a scanning speed of 2 cm^{-1}/s with 5-cm^{-1} resolution. Data were collected using backscattering geometry with spinning catalyst pellets.

X-ray photoelectron spectra were obtained with an AEI 200B spectrometer using Al$K\alpha$ radiation. All spectra are referenced to a carbon 1*s* binding energy of 284.6 eV. Air contamination of the samples was avoided by opening all synthesis tubes and the reactor in a nitrogen dry box. Samples for XPS analysis were sealed inside Pyrex tubes which were opened in a helium dry box attached directly to the spectrometer. Fresh catalyst samples were obtained immediately after the synthesis tubes were opened. Samples of used catalysts were obtained from a 40–100 mesh portion removed from the reactor with no further grinding.

RESULTS

a. Activity Measurements

The continuous-flow thiophene reaction results for the Chevrel phases after 20 min and 10 h of reaction are summarized in Table 1. The empty reactor converted 0.3% of the thiophene to C_4 products, and this value was subtracted from the C_4 yields before the HDS activities were calculated. All catalysts had an increase in surface area after 10 h of reaction. Therefore, the initial surface areas were used to normalize the HDS activities after 20 min of thiophene reaction while the activities after 10 h of reaction were normalized using the final surface areas. After 10 h of thiophene HDS, most materials showed a decrease in activity (*35*), except for $Lu_{1.2}Mo_6S_8$ and $Lu_{0.8}Pb_{0.33}Mo_6S_8$ which showed a slight increase. The C_4 hydrocarbon product distributions resulting from thiophene HDS varied with the cata-

TABLE 1

Thiophene Hydrodesulfurization (HDS) Activities (400°C)

Catalyst (formal Mo oxidation state)	Surface area (m^2/g)	Reaction time	Thiophene conversion (%)	HDS rate (mol/s · m^2) × 10^8	C_4 product distribution (%)			
					n-Butane	1-Butene	*trans*-2-Butene	*cis*-2-Butene
$Lu_{1.2}Mo_6S_8$ (2.07)	0.693	20 min	2.06	1.80	3.6	37.3	34.7	24.4
	1.093	10 h	3.48	1.93	3.0	28.6	40.0	28.4
$Lu_{0.8}Pb_{0.33}Mo_6S_8$ (2.16)	0.689	20 min	1.64	1.55	2.3	44.1	32.4	21.2
	1.033	10 h	3.17	2.00	0.7	34.7	38.8	25.8
$Lu_{0.4}Pb_{0.67}Mo_6S_8$ (2.24)	0.563	20 min	1.59	4.43	1.3	48.4	31.9	18.4
	0.644	10 h	1.36	3.30	—[a]	47.9	34.3	17.8
$PbMo_{6.2}S_8$ (2.26)	1.318	20 min	1.59	4.53	—[a]	65.5	20.2	14.3
	1.664	10 h	1.16	2.61	—[a]	65.6	21.8	12.6
$Lu_{0.1}PbMo_6S_8$ (2.28)	0.649	20 min	2.60	8.43	0.8	53.5	26.7	19.0
	0.952	10 h	2.84	6.27	0.6	55.0	25.5	18.9

[a] Below detection limit.

lysts. The ratio of 2-butenes to 1-butene after 10 h of reaction was 2.4 for $Lu_{1.2}Mo_6S_8$, 1.9 for $Lu_{0.8}Pb_{0.33}Mo_6S_8$, 1.0 for $Lu_{0.4}Pb_{0.67}Mo_6S_8$, 0.81 for $Lu_{0.1}PbMo_6S_8$, and 0.52 for $PbMo_{6.2}S_8$. These values differed from the thermodynamic equilibrium value at 400°C for which the ratio of 2-butenes to 1-butene is about 2.8 (*48*).

The 1-butene HYD activities were normalized on the basis of the initial surface areas and calculated as the rate of production of *n*-butane. The results are presented in Table 2. The empty reactor produced 0.06% *n*-butane, and this value was subtracted from the *n*-butane yields before the activities were calculated. The activities are reported for three different times: (A) fresh catalyst, (B) after 25 H_2–thiophene pulses, and (C) after 2 h continuous-flow thiophene reaction. $Lu_{0.1}PbMo_6S_8$ showed no ability to hydrogenate 1-butene. All other catalysts showed an increase in HYD activity after 2 h of continuous-flow thiophene reaction. This may indicate a necessary period of activation for these materials toward the hydrogenation of 1-butene. No detectable cracking products were observed. The HYD activity experiments also indicate the ability of the catalysts to isomerize 1-butene to *trans*-2-butene and *cis*-2-butene. A considerable departure from the thermodynamic equilibrium value at 400°C was noted for all catalysts. After 2 h of thiophene reaction, 62% of the 1-butene was unconverted for $Lu_{1.2}Mo_6S_8$ compared to 46% for $PbMo_{6.2}S_8$. For thermodynamic equilibrium at 400°C, about 26.5% 1-butene would be observed (*48*).

b. Catalyst Characterization

A representative X-ray powder diffraction pattern of the catalysts used in this work is shown in Fig. 1. The powder diffraction peaks were indexed on the basis of a rhombohedral unit cell. The data show $Lu_{0.1}PbMo_6S_8$ before and after 10 h of thiophene reaction with no apparent change in the X-ray pattern. This result was typical for all of the Chevrel phases studied and indicates no loss in crystallinity and no formation of other phases or impurities.

Raman spectra could not be obtained for the Chevrel phases, but MoS_2 impurities can be detected using this technique. Raman spectroscopy is a sensitive probe for both crystalline and poorly crystalline MoS_2 (bands at 383 and 409 cm^{-1}) (*49–50*). The Raman spectra for all of the Chevrel phases used in this study are devoid of any MoS_2 features, for fresh catalysts and for catalysts after 10 h of thiophene reaction.

Representative X-ray photoelectron spectra for the catalysts are shown in Fig. 2 ($Lu_{1.2}Mo_6S_8$ before and after 10 h continuous-flow H_2–thiophene reaction). A nonlinear least-squares curve-fitting program was

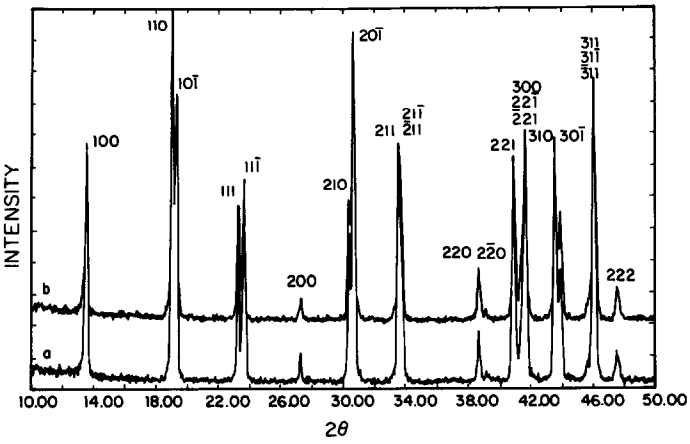

FIG. 1. X-ray powder diffraction pattern of (a) fresh and (b) used (10 h of thiophene reaction) $Lu_{0.1}PbMo_6S_8$ with rhombohedral *hkl* indexes.

used to analyze the spectra (*51*). The contribution of the sulfur 2*s* signal at lower binding energies (225.5 eV) was eliminated using this program. Two components with a peak separation between the Mo $3d_{5/2}$ and $3d_{3/2}$ lines of 3.2 eV were required to fit the molybdenum data region. The curve-fitting procedure revealed the presence of a small amount of a molybdenum-containing impurity with $3d_{5/2}$ and $3d_{3/2}$ binding energies of 231.4 and 234.6 eV, respectively. These binding energies are indicative of MoO_2

TABLE 2

1-Butene Hydrogenation (HYD) Activities (400°C)

Catalyst (formal Mo oxidation state)		HYD rate (mol/s · m²) × 10⁹	C_4 product distribution (%)			
			n-Butane	1-Butene	*trans*-2-Butene	*cis*-2-Butene
$Lu_{1.2}Mo_6S_8$ (2.07)	A	0.23	0.03	91.7	3.5	4.7
	B	0.38	0.05	92.8	3.1	4.0
	C	0.91	0.12	62.3	20.4	17.1
$Lu_{0.8}Pb_{0.33}Mo_6S_8$ (2.16)	A	0.28	0.03	89.2	5.1	5.7
	B	0.09	0.01	88.6	5.5	5.8
	C	0.83	0.09	59.6	21.5	18.8
$Lu_{0.4}Pb_{0.67}Mo_6S_8$ (2.24)	A	0.22	0.01	74.8	12.6	12.6
	B	0.66	0.03	61.6	19.9	18.5
	C	0.88	0.04	54.3	24.1	21.5
$PbMo_{6.2}S_8$ (2.26)	A	0.24	0.01	89.1	5.6	5.3
	B	0.24	0.01	59.5	21.8	18.6
	C	1.20	0.05	46.2	28.6	25.2
$Lu_{0.1}PbMo_6S_8$ (2.28)	A	0.00	0.0	93.7	3.4	2.9
	B	0.00	0.0	86.9	6.9	6.2
	C	0.00	0.0	88.3	5.3	6.4
Calculated butene equilibrium at 400°C[a]				26.5	43.5	30.0

Note. A, fresh catalyst; B, after 25 H_2–thiophene pulses; C, after 2 h of continuous H_2–thiophene reaction.
[a] See Ref. (*48*).

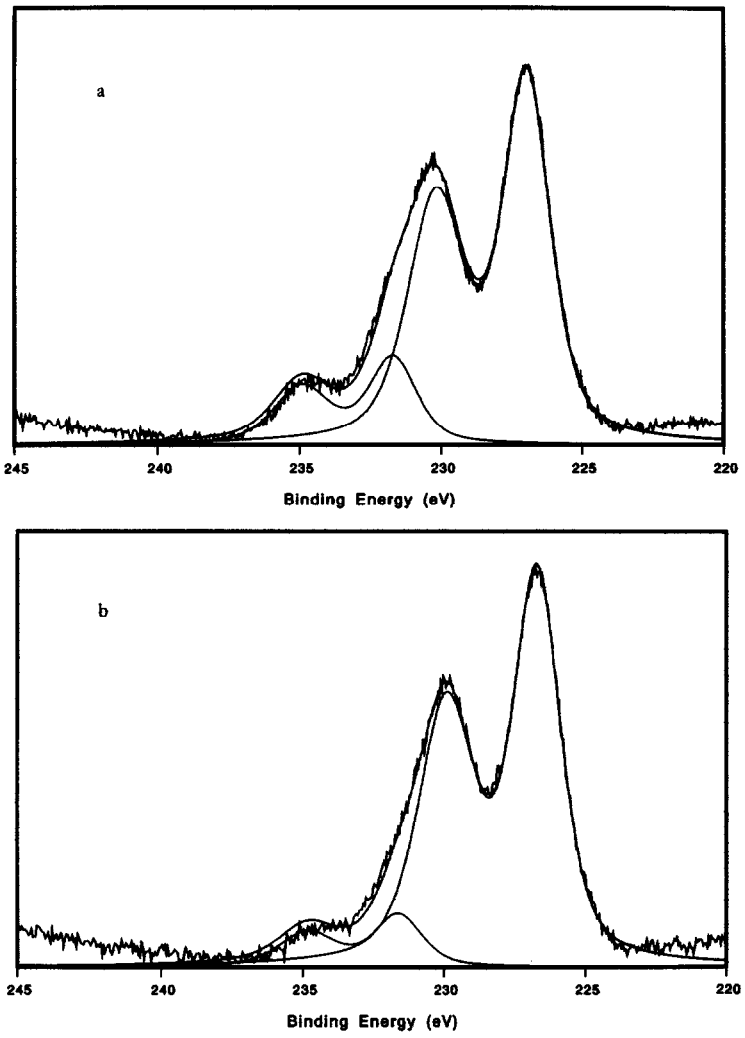

FIG. 2. Molybdenum 3*d* XPS spectra of (a) fresh and (b) used (10 h of thiophene reaction) $Lu_{1.2}Mo_6S_8$.

(*52–53*) which presumably was formed by the high-temperature reaction of the Chevrel phases with the fused-silica tubes (*47*). Similarly, Swartz and Hercules have reported that the surface oxidation of molybdenum powder results in the formation of MoO_2 rather than MoO_3 (*52*). A comparison of the MoO_2 peaks for the fresh (Fig. 2a) and used (Fig. 2b) catalyst demonstrates that a decrease in signal intensity by a factor of 2 occurs. This trend was observed for all Chevrel phases examined in this study.

The XPS data for all catalysts are summarized in Table 3. The binding energies were calculated from the actual XPS data without the use of the curve-fitting procedure. For comparison, the $3d_{5/2}$ binding energy for Mo^{4+} in MoS_2 is about 228.9 eV, and that for Mo^{6+} is about 232.5 eV (*4*). Basically, there were no significant shifts in the molybdenum 3*d* binding energies after 10 h continuous-flow H_2–thiophene reaction; some small shifts to lower binding energies (observed for only some of the catalysts) were due to the reduction of MoO_2.

TABLE 3

XPS Binding Energies and Intensity Ratios

Catalyst		Binding energies (eV)							Calculated ratios		
		Mo		Pb		Lu		S	Pb/Mo[a]	Lu/Mo[b]	S/Mo[c]
		$3d_{3/2}$	$3d_{5/2}$	$4f_{5/2}$	$4f_{7/2}$	$4d_{3/2}$	$4d_{5/2}$	$2p$			
$Lu_{1.2}Mo_6S_8$	A	231.1	227.7	n/a[d]	n/a	207.0	197.2	161.8	n/a[d]	0.17	0.33
	B	230.8	227.6	n/a	n/a	206.3	196.6	161.8	n/a	0.91	0.30
$Lu_{0.8}Pb_{0.33}Mo_6S_8$	A	230.9	227.4	142.8	137.8	207.2	197.4	162.0	0.23	0.11	0.32
	B	230.8	227.6	142.6	137.9	207.0	197.3	162.2	0.20	0.19	0.32
$Lu_{0.4}Pb_{0.67}Mo_6S_8$	A	231.4	228.1	142.5	137.8	207.3	197.6	161.9	0.31	0.06	0.33
	B	231.0	227.6	142.6	137.8	207.0	197.2	161.9	0.30	0.18	0.37
$PbMo_{6.2}S_8$	A	231.1	227.8	143.3	138.6	n/a[d]	n/a	162.3	0.50	n/a[d]	0.33
	B	231.0	227.8	143.0	138.3	n/a	n/a	162.4	0.40	n/a	0.42
$Lu_{0.1}PbMo_6S_8$	A	231.5	228.1	143.3	138.6	—[e]	—	162.2	0.48	—[e]	0.33
	B	231.1	227.8	142.8	138.0	—	—	162.2	0.48	—	0.37

Note. A, fresh catalyst; B, after 10 h of continuous H_2–thiophene reaction.
[a] Raw area ratio of Pb $4f$ electrons to Mo $3d$ electrons.
[b] Raw area ratio of Lu $4d$ electrons to Mo $3d$ electrons.
[c] Raw area ratio of S $2p$ electrons to Mo $3d$ electrons.
[d] Not applicable.
[e] Lu concentration too low to evaluate.

The molybdenum $3d_{5/2}$ binding energies for the fresh catalysts are grouped around 227.8 eV, ranging from 228.1 for $Lu_{0.4}Pb_{0.67}Mo_6S_8$ and $Lu_{0.1}PbMo_6S_8$ to 227.4 eV for $Lu_{0.8}Pb_{0.33}Mo_6S_8$. These results confirm the anticipated low oxidation states for molybdenum. Due to the presence of varying amounts of MoO_2 incorporated in the catalysts and the resultant peak broadening, the molybdenum $3d_{5/2}$–$3d_{3/2}$ peak separations varied slightly.

Table 3 also shows the ratios of the raw peak areas for the lead $4f$ and lutetium $4d$ electrons compared to the molybdenum $3d$ electrons. These ratios are not intended to quantitatively reflect the surface compositions since they are not corrected for instrumental or atomic sensitivity factors. Rather, they are intended to indicate changes in the surface compositions which occur after thiophene reaction. The ratio of surface lead atoms to surface molybdenum atoms remained approximately the same under the reaction conditions. However, the ratio of surface lutetium atoms to surface molybdenum atoms increased significantly relative to the fresh catalysts after 10 h of thiophene reaction. The delocalization of the ternary atoms from their crystallographic positions in the Chevrel phase structure is related to the movement of the ternary metal. This delocalization is strong for small cations resulting in high mobilities; in contrast large cations have low mobilities in the crystal lattice (*42*). Lutetium atoms apparently migrate from the bulk to the surface of the catalyst under reaction conditions. Because of the difficulty in quantifying the surface concentrations, it was unrealistic to calculate molybdenum formal oxidation states based on an estimate of the stoichiometry at the surface.

DISCUSSION OF RESULTS

Previous investigations with Chevrel phases have demonstrated that these materials have thiophene HDS activities comparable to—or greater than—model unpromoted and cobalt-promoted MoS_2-based catalysts (*33–35*). In this study the effect of a systematic variation in molybdenum oxidation state on catalytic activity for thiophene HDS was examined using a series of lead–lutetium Chevrel phases. By using this substitutional series of compounds, the formal oxidation state of molybdenum

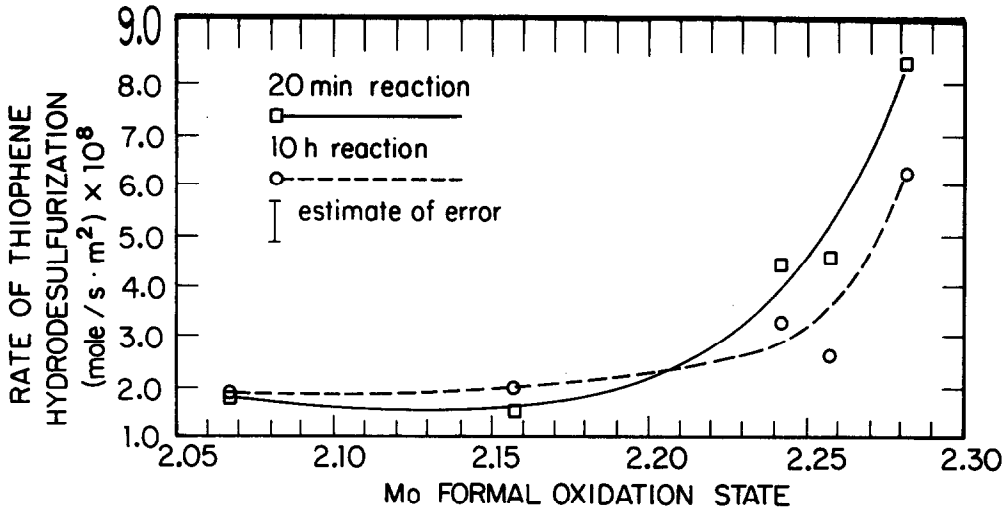

FIG. 3. Thiophene hydrodesulfurization activities (400°C) as a function of the formal oxidation state of molybdenum for 20 min and 10 h of thiophene reaction.

could be directly controlled either by inserting Lu^{3+} into $PbMo_6S_8$ or by substituting Lu^{3+} for Pb^{2+} in the Chevrel phase structure. The Chevrel phases can be referred to as reduced molybdenum sulfides (compared to MoS_2) and are known to possess a metallic nature; ternary components such as Pb and Lu can transfer valence electrons to the Mo_6 octahedral (cluster) units (*42–43*). The extent of the charge transfer can be altered by varying the concentration of the ternary component or by using ternary components with different valences. This results in a change in the formal oxidation state of the molybdenum.

Figure 3 illustrates the trends for the rate of thiophene HDS versus the formal oxidation state of molybdenum for 20-min and 10-h reaction times. The formal oxidation state of molybdenum was calculated from the nominal stoichiometries by assuming valences of Lu^{3+}, Pb^{2+}, and S^{2-}. Previous work with an unpromoted MoS_2 catalyst (Mo^{4+}) has determined thiophene HDS rates of 2.67×10^{-8} and 0.92×10^{-8} mol/s · m^2 for 20-min and 10-h reaction times, respectively (*35*). Considering all of these data, it is possible to propose a general correlation of thiophene HDS activity and molybdenum formal oxidation state. Specifically, the rate of thiophene HDS apparently approaches a maximum between the highest molybdenum oxidation state (+2.28) for the Chevrel phase catalyst and the molybdenum oxidation state (+4) for MoS_2. Of course, it is not possible to eliminate all structural and compositional effects on HDS activity in comparing these compounds. These factors have been shown to exist for Chevrel phases (*38*) and MoS_2-based catalysts. It should be noted that it is not possible to prepare a Chevrel phase with a molybdenum formal oxidation state near +3. The highest molybdenum oxidation state attainable for Chevrel phases is $+2\frac{2}{3}$ corresponding to the binary compound Mo_6S_8. This material, however, decomposes at about 400°C (*54*) and forms large amounts of MoS_2 during thiophene HDS at 300°C for 2 h (*35*).

XPS analysis indicated that the molybdenum oxidation states at the surface of the Chevrel phase catalysts were indeed reduced compared to MoS_2. Oxidation of molybdenum in the surface regions could not be appreciably observed after 10 h of thiophene reaction. The XPS data did, however, reveal some degree of ternary metal delocalization due to the reaction conditions. Lead, a large cation, demonstrated

the expected low mobility, but lutetium appeared to migrate to some small degree from the bulk to the surface. The oxidation state of surface molybdenum apparently either is unaffected by this limited migration or perhaps becomes very slightly reduced.

Experimental and theoretical evidence for an electronic theory of HDS catalysis has been offered by several research groups. Harris (*29–30*) has provided an SCF–SW–Xα method for modeling the energy levels and charge distributions for MS_6^{n-} (first-row transition metals M = Ti–Ni and second-row transition metals M = Zr–Pd) clusters and $MoM'S_9^{n-}$ (first-row transition metal "promoters" M' = V–Zn) clusters. These calculations are consistent with the XPS spectra of the sulfides and indicate that bonding in the 4*d* transition-metal sulfides is considerably more covalent than in the 3*d* sulfides. The activity of the unpromoted transition-metal clusters (sulfides) for dibenzothiophene HDS activity was correlated with the orbital occupation of the highest occupied molecular orbital (HOMO) and the metal–sulfur covalent-bond strength (*31*). The role of the promoters for molybdenum clusters was to affect the number of electrons in the HOMO, that is, the number of *d* electrons on molybdenum. For Co–Mo and Ni–Mo clusters, the number of electrons is increased by the presence of the promoter; Cu has the opposite effect. These calculations also correlate with the activity for dibenzothiophene HDS activity (*32*): Co and Ni are excellent promoters while Cu acts as a poison. Vissers *et al.* (*55*) also report a correlation between thiophene HDS activity for second- and third-row transition metals and the shift in XPS binding energies between metal and metal sulfide phases. The most active transition-metal sulfides were observed to preserve their metallic character in the sulfide phase under reaction conditions. Specifically, these materials were proposed to be sulfur-deficient, highly reduced sulfides having valence electrons in the metal–sulfur molecular orbitals which maintain their metal character.

Chevrel phases are part of a group of "metal-rich" compounds including halides, oxides, and other ligands. For Chevrel phases the fundamental cubic structure is defined by the presence of Mo_6S_8 units consisting of a molybdenum cluster or octahedron. The Mo–Mo bond distances within a cluster are relatively short, typically in the range of 2.65–2.80 Å, compared to 2.72 Å for metallic Mo (*40*). The Mo_6 cluster is capable of playing an electron donor–acceptor role (*43*). The Mo_6S_8 compound (no ternary metal) is the most electron-poor compound ($20e^-$ per Mo_6 cluster) with electron-deficient Mo–Mo bonds; it is a metastable compound. The addition of ternary metals adds electrons to the cluster and stabilizes the cluster unit. The Mo–Mo bond distance becomes shorter, and the octahedron becomes regular for $24e^-$ per Mo_6 cluster. The high catalytic activity of the Chevrel phases correlates with the metallic or "reduced" nature of these sulfides: indeed, by comparing the activity to conventional MoS_2-based catalysts, one finds that higher activity is obtained when the molybdenum formal oxidation state is reduced below Mo^{4+}. The results of our work indicate that a maximum in activity may exist between Mo^{2+} and Mo^{4+}.

The observation of a maximum in the rate of thiophene HDS is not unexpected. Recent kinetic measurements have indicated that thiophene adsorption and reaction with surface nucleophiles (to produce dihydrothiophene intermediates) are likely the rate-limiting steps in HDS (*56–57*). Although the adsorption state of thiophene is still unclear, η^5-binding apparently would give rise to C–S bond weakening (*58*). Thiophene is more likely to bond to metals in the lower oxidation state based on an analysis of model organometallic compounds (*59*). However, nucleophilic attack to produce hydrogenated intermediates (2,3-dihydrothiophene and 2,5-dihydrothiophene), which are highly reactive to-

ward HDS, would be promoted by sulfides in higher molybdenum oxidation states. This may explain why a maximum is observed in considering Fig. 3 and the data for typical MoS_2-based catalysts.

Consistent with this observation is the low activity of the Pb–Lu Chevrel phases for 1-butene hydrogenation. This is not unexpected since similar results have been reported for other Chevrel phases (*33–35*). For comparison, model unpromoted and cobalt-promoted MoS_2-based catalysts have 1-butene HYD activities of 7.5×10^{-9} and 7.1×10^{-9} mol/s · m^2 after 2 h of thiophene HDS, respectively. The Chevrel phases do exhibit an increase in 1-butene HYD following 2 h of continuous thiophene HDS; however, this activity is still approximately eight times lower than the model MoS_2-based materials. Undoubtedly some of this effect is due to the migration of Lu atoms to the surface. The XPS data, however, indicated little effect on the molybdenum oxidation state.

CONCLUSIONS

The thiophene HDS activities of the lead–lutetium series Chevrel phase catalysts investigated were found to be comparable to those of previously examined Chevrel phases and to those of model unpromoted and cobalt-promoted MoS_2 catalysts, indicating that they are potentially useful HDS catalysts. These materials also demonstrated low 1-butene HYD activities making them rather selective catalysts. The bulk structures and the reduced surface molybdenum oxidation states have been determined to be stable under reaction conditions. It was possible to relate catalyst activity to the formal oxidation state of molybdenum for these compounds; thiophene HDS activity is associated with "reduced" molybdenum oxidation states, apparently reaching a maximum between Mo^{2+} and Mo^{4+}.

ACKNOWLEDGMENTS

This work was conducted through the Ames Laboratory which is operated for the U.S. Department of Energy by Iowa State University under Contract W-7405-Eng-82. This research was supported by the Office of Basic Energy Sciences, Chemical Sciences Division.

REFERENCES

1. Grange, P., *Catal. Rev. Sci. Eng.* **21,** 135 (1980).
2. Wivel, C., Candia, R., Clausen, B. S., Mørup, S., and Topsøe, H., *J. Catal.* **68,** 453 (1981).
3. Bachelier, J., Duchet, J. C., and Cornet, D., *J. Catal.* **87,** 283 (1984).
4. Li, C. P., and Hercules, D. M., *J. Phys. Chem.* **88,** 456 (1984).
5. Zingg, D. S., Makovsky, L. E., Tisher, R. E., Brown, F. R., and Hercules, D. M., *J. Phys. Chem.* **84,** 2898 (1980).
6. Patterson, T. A., Carver, J. C., Leyden, D. E., and Hercules, D. M., *J. Phys. Chem.* **80,** 1700 (1976).
7. Parham, T. G., and Merrill, R. P., *J. Catal.* **85,** 295 (1984).
8. Pollack, S. S., Makovsky, L. E., and Brown, F. R., *J. Catal.* **59,** 452 (1979).
9. Schrader, G. L., and Cheng, C. P., *J. Catal.* **80,** 369 (1983).
10. Okamoto, Y., Shimokawa, T., Imanaka, T., and Teranishi, S., *J. Catal.* **57,** 153 (1979).
11. Furimsky, E., *Catal. Rev. Sci. Eng.* **22,** 371 (1980).
12. Topsøe, H., Clausen, B. S., Wivel, C., and Mørup, S., *J. Catal.* **68,** 433 (1981).
13. Topsøe, H., Candia, R., Topsøe, N. Y., and Clausen, B. S., *Bull. Soc. Chim. Belg.* **93,** 783 (1984).
14. Delvaux, G., Grange, P., and Delmon, B., *J. Catal.* **56,** 99 (1979).
15. Alstrup, I., Chorkendorff, I., Candia, R., Clausen, B. S., and Topsøe, H., *J. Catal.* **77,** 397 (1982).
16. Voorhoeve, R. J. H., *J. Catal.* **23,** 236 (1971).
17. Konings, A. J. A., Valster, A., de Beer, V. H. J., and Prins, R., *J. Catal.* **76,** 466 (1982).
18. Thakur, D. S., and Delmon, B., *J. Catal.* **91,** 308 (1985).
19. Bachelier, J., Duchet, J. C., and Cornet, D., *Bull. Soc. Chim. Belg.* **90,** 1301 (1981).
20. Tauster, S. J., Pecoraro, T. A., and Chianelli, R. R., *J. Catal.* **63,** 515 (1980).
21. Jung, H. J., Schmitt, J. L., and Ando, H., *in* "Proceedings of the Climax Fourth International Conference on Chemistry and Uses of Molybdenum" (H. F. Barry and P. C. H. Mitchell, Eds.), p. 246. Climax Molybdenum Co., Ann Arbor, MI, 1982.
22. Segawa, K. I., and Hall, W. K., *J. Catal.* **77,** 221 (1983).
23. Valyon, J., and Hall, W. K., *J. Catal.* **84,** 216 (1983).
24. Delgado, E., Fuentes, G. A., Hermann, C., Kunzmann, G., and Knözinger, H., *Bull. Soc. Chim. Belg.* **93,** 735 (1984).

25. Bachelier, J., Tilliette, M. J., Cornac, M., Duchet, J. C., Lavalley, J. C., and Cornet, D., *Bull. Soc. Chim. Belg.* **93,** 743 (1984).
26. Peri, J. B., *J. Phys. Chem.* **86,** 1615 (1982).
27. Laine, J., Severino, F., Cáceres, C. V., Fierro, J. L. G., and Lopez Agudo, A., *J. Catal.* **103,** 228 (1987).
28. Duben, A. J., *J. Phys. Chem.* **82,** 348 (1978).
29. Harris, S., *Chem. Phys.* **67,** 229 (1982).
30. Harris, S., *Polyhedron* **5,** 151 (1986).
31. Harris, S., and Chianelli, R. R., *J. Catal.* **86,** 400 (1984).
32. Harris, S., and Chianelli, R. R., *J. Catal.* **98,** 17 (1986).
33. McCarty, K. F., and Schrader, G. L., *in* "Proceedings, 8th International Congress on Catalysis, Berlin, 1984," Vol. IV, p. 427. Dechema, Frankfurt-am-Main, 1984.
34. McCarty, K. F., and Schrader, G. L., *Ind. Eng. Chem. Prod. Res. Dev.* **23,** 519 (1984).
35. McCarty, K. F., Anderegg, J. W., and Schrader, G. L., *J. Catal.* **93,** 375 (1985).
36. McCarty, K. F., and Schrader, G. L., *J. Catal.* **103,** 261 (1987).
37. Huckett, S. C., Angelici, R. J., Ekman, M. E., and Schrader, G. L., *J. Catal.* **113,** 36 (1988).
38. Schrader, G. L., and Ekman, M. E., *in* "Advances in Hydrotreating Catalysts" (M. L. Occelli and R. Anthony, Eds.), in press. Elsevier, Amsterdam.
39. Chevrel, R., Sergent, M., and Prigent, J., *J. Solid State Chem.* **3,** 515 (1971).
40. Chevrel, R., and Sergent, M., *in* "Topics in Current Physics" (Ø. Fischer and M. B. Maple, Eds.), Vol. 34, p. 25. Springer-Verlag, Berlin, 1982.
41. Yvon, K., *in* "Topics in Current Physics" (Ø. Fischer and M. B. Maple, Eds.), Vol. 34, p. 87. Springer-Verlag, Berlin, 1982.
42. Yvon, K., *in* "Current Topics in Materials Science" (E. Kaldis, Ed.), Vol. 3, p. 53. North-Holland, Amsterdam, 1979.
43. Chevrel, R., Hirrien, M., and Sergent, M., *Polyhedron* **5,** 87 (1986).
44. Tarascon, J. M., DiSalvo, F. J., Murphy, D. W., Hull, G. W., Rietman, E. A., and Waszczak, J. V., *J. Solid State Chem.* **54,** 204 (1984).
45. Sergent, M., Chevrel, R., Rossel, C., and Fischer, Ø., *J. Less-Common Met.* **58,** 179 (1978).
46. Flükiger, R., and Baillif, R., *in* "Topics in Current Physics" (Ø. Fischer and M. B. Maple, Eds.), Vol. 34, p. 113. Springer-Verlag, Berlin, 1982.
47. Miller, W. M., and Ginsberg, D. M., *Phys. Rev. B* **28,** 3765 (1983).
48. Benson, S. W., and Bose, A. W., *J. Amer. Chem. Soc.* **85,** 1385 (1963).
49. Chang, C. H., and Chan, S. S., *J. Catal.* **72,** 139 (1981).
50. Wieting, T. J., and Verble, J. L., *Phys. Rev. B* **3,** 4286 (1971).
51. Luly, M. H., "APES—A FORTRAN Program to Analyze Photoelectron Spectra." Ames Laboratory, DOE, Iowa State University, Ames, 1979.
52. Swartz, W. E., and Hercules, D. M., *Anal. Chem.* **43,** 1774 (1971).
53. Brox, B., and Olefjord, I., *Surf. Interface Anal.* **13,** 3 (1988).
54. Cheung, K. Y., and Steele, B. C. H., *Solid State Ionics* **1,** 337 (1980).
55. Vissers, J. P. R., Groot, C. K., van Oers, E. M., de Beer, V. H. J., and Prins, R., *Bull. Soc. Chim. Belg.* **93,** 813 (1984).
56. Markel, E. J., Schrader, G. L., Sauer, N. N., and Angelici, R. J., *J. Catal.*, in press.
57. Sauer, N. N., Markel, E. J., Schrader, G. L., and Angelici, R. J., *J. Catal.*, in press.
58. Zonnevylle, M. C., Hoffmann, R., and Harris, S., *Surf. Sci.* **199,** 320 (1988).
59. Angelici, R. J., *Acc. Chem. Res.* **21,** 387 (1988).